Power Grid Frequency Forecasting from μPMU Data using Hybrid Vector-Output LSTM network

1st Maitreyee Dey
Neuville Grid Data Ltd,
London South Bank University,
London, UK

2nd Dilshan Wickramarachchi
School of Engineering,
London South Bank University,
London, UK

3rd Soumya P. Rana
Sensing Imaging and Signal Processing Group
University of Manchester
Manchester, UK

4th Clarke V Simmons
Neuville Grid Data Ltd,
London, UK

5th Sandra Dudley
School of Engineering,
London South Bank University,
London, UK

***Abstract*—The instantaneous balance of electrical supply and demand on the power grid is indicated by the power grid frequency, making it a pivotal variable for power system controls. Accurate frequency forecasting could enable new faster means of frequency management that enhance power system stability. A hybrid vector-output Long Short-Term Memory (LSTM) neural network has been studied using microsynchrophasor data to predict trajectories. The objective of this research is to evaluate the effectiveness of very short time horizon frequency prediction using this method. The proposed model has been trained with over and under-frequency operational limit excursion events as well as normal condition state, with the goal of minimising prediction errors. Training and testing have been conducted using 390,000 datapoints covering 65 frequency events obtained from a distribution grid connected solar farm in England. The results demonstrate this method can provide useful grid frequency projections and shed light on underlying behaviour.**

***Index Terms*—Electrical grid frequency, power system stability, time series forecasting, long short term memory.**

I. Introduction

Transmission and Distribution system operators face a significant challenge in maintaining the stability and control of the nominal grid frequency (50/60 Hz). Asynchronous Renewable Energy Generation (REG) and power electronics-based loads are becoming more prevalent in many electrical power systems, while centralised synchronous power generators and rotating electrical machinery are declining. One significant disadvantage of REG, such as utility-scale solar photovoltaic (PV) installations with their grid following inverters, is their inability to contribute to system inertia since they are not synchronous sources of generation [1].

Grid stability can be measured by several factors, including frequency stability, voltage stability, and angular stability; all of which are important to ensuring the resilience and reliability of the power grid to perturbations. This is especially important during periods of high penetration of asynchronous renewable energy generation and low demand, which can result in low levels of system inertia and grid instability [2]. If there are insufficient levels of inertia in a power system and they are not properly managed, it can result in interruptions to power supply or a degradation of power quality. This can ultimately impact the grid's reliability and, in severe cases, cause brownouts or even blackouts [3].

Grid frequency is highly dynamic and it requires close monitoring. It is essential to maintain the system frequency within both the statutory and operational limits of a given grid; in the UK, these limits are 49.5-50.5Hz and 49.8-50.2Hz respectively. The National Grid Energy System Operator (NGESO) has identified frequency management as a top challenge. [4].

Presently, system operators rely on Supervisory Control And Data Acquisition (SCADA) systems to collect and monitor frequency data. However, these systems usually provide relatively coarse data from a limited number of nodes and this is inadequate for addressing rising challenges of electrical networks undergoing rapid transformation [5].

The microsynchrophasor measurement unit (μPMU) was created specifically for distribution grids and it overcomes some of the limitations associated with conventional Phasor Measurement Units (PMU) and legacy SCADA systems [6]. The μPMU complies with the IEEE C37.118.2-2011 standard and it features a Total Vector Error (TVE) of $\pm 0.01\%$ and an angular accuracy of $\pm 0.003^o$, which is significantly better than the 1.0% TVE common to conventional PMUs found on transmission systems [6].

The μPMU is capable of collecting vast amounts of highly accurate voltage and current phasor data, making it ideal for monitoring network event behaviour. However, due to the diverse range of distribution network events, it can be challenging to categorise different frequency events [7]. Without prior knowledge of categorised and encoded grid behaviour, converting μPMU measurements into actionable information during real-life scenarios remains a significant challenge.

Several machine learning (ML) techniques have been employed in literature to predict power grid frequency [8]. In [9],

979-8-3503-9678-2/23/.00

weighted-nearest neighbour method was used to forecast power grid frequency with one-second resolution data, predicting one hour ahead. However, this method is constrained by data availability. Djukanovic et. al. used artificial neural networks (ANNs) to forecast short-term dynamic frequency in the New England power system, with inputs obtained through a series of calculations based on initial facility data. [10]. Zhang et al. proposed a LSTM encoder-decoder model to predict dynamic sequence in frequency, achieving an Root Mean Square Error (RMSE) of 0.0205 for 0.01sec input sequence [11]. In another study, a convolutional long short-term memory (ConvLSTM) network was used for frequency prediction using simulated data, taking four different input parameters into account (voltage phase angle, generator electromagnetic power, active load power, and generator rotor speed) [12]

In this paper, high-resolution μPMU frequency data from a utility-scale solar PV site has been gathered and a hybrid vector output LSTM model employed for multi-step univariate frequency forecasting. The results demonstrate precise forecasting of near-future frequency data trajectories and enhance our fundamental understanding of power grid frequency behaviour.

The rest of the paper is organised as follows. Section II describes the methods and material used for developing the algorithm. Section III presents the details of the data and discussion of the result followed by Section IV containing the conclusion drawn.

II. Methods & Materials

The research had two stages: the first stage was gathering a significant amount of μPMU frequency data and the second stage focused on utilising deep neural network-based techniques to forecast the frequency up to one second ahead. A framework of the proposed steps of this work is shown in Fig. 1.

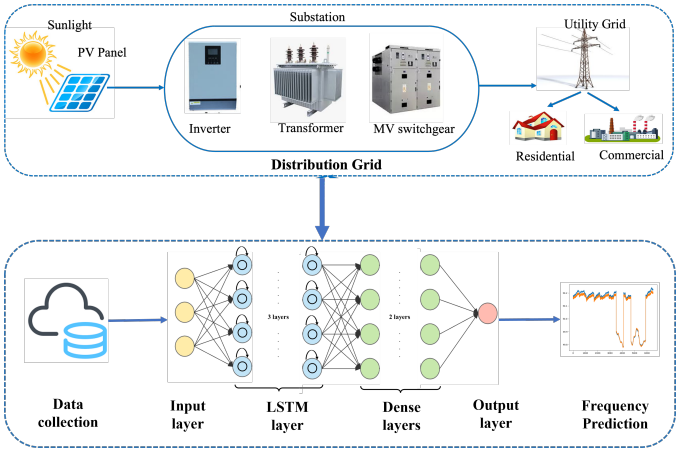

Fig. 1: Flow diagram of the proposed architecture.

A. Data Collection and Processing

Neuville Grid Data (NGD) was responsible for collecting the μPMU data, using their Grid Data Unit (GDU) [13]. The GDU is a patented apparatus that integrates a μPMU, Power Quality Monitor (PQM), Global Positioning System (GPS) based timing for sub-100 nanosecond time synchronisation, data-buffering memory, edge computing, and secure bidirectional 3G/4G cellular data telemetry. The μPMU and PQM digital signal processing (DSP) instruments receive analogue signals from instrument transformers, enabling the device to determine both current and voltage phasors twice per AC cycle (100Hz in Britain) for all three phases and provide an accurate estimation of frequency [14], [15].

B. Hybrid Vector Output Long Short Term Memory

In this research, a hybrid vector output LSTM neural netowrk was proposed for power grid frequency prediction. It incorporates feedback connections, making it suitable for processing data sequences and time-series prediction. The model comprises of three LSTM layers followed by two dense layers. Two dropout layers have also been included to enhance the training process as illustrated in Fig. 2.

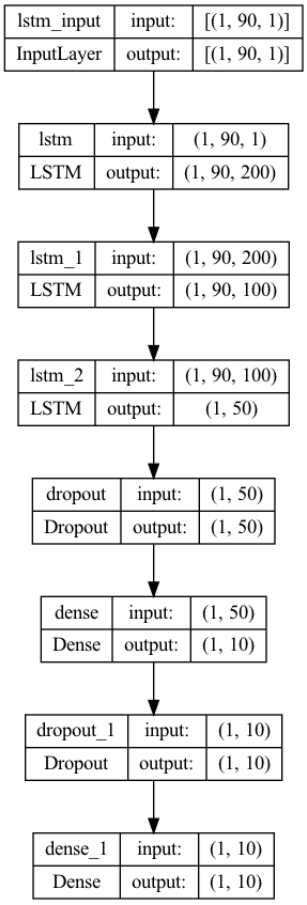

Fig. 2: The employed LSTM architecture of this study.

The LSTM input frequency data underwent pre-processing normalisation due to a higher mean frequency of 49.96 Hz

compared to a lower standard deviation of 0.058 Hz. The input frequencies (F) were normalised to a range from 0 to 1 using min-max normalisation (F_{norm}), as shown in Eq. (1). This normalisation pre-processing is necessary to ensure that the input data is on a consistent scale highlighting the frequency changes to improve the effectiveness of the LSTM model.

$$F_{norm} = (F - F_{\min})/(F_{max} - F_{\min}) \tag{1}$$

The working principle of the LSTM layers is shown in Eq. (2) to (7) [16], where input is x_t, W_f, W_i, W_C, and W_O refers to the input weight, and the g refers to the activation function. The b_f, b_i, b_C and b_O are the biases. The t and $t-1$ denote the current and previous time stamps. The x and h represent the input and output, and C represents the cell status.

$$f(t) = g(W_f \cdot [h_{t-1}, x_t] + b_f) \tag{2}$$

$$i(t) = g(W_i \cdot [h_{t-1}, x_t] + b_i) \tag{3}$$

$$\tilde{C}(t) = tanh(W_c \cdot [h_{t-1}, x_t] + b_c) \tag{4}$$

$$C(t) = f_t * C_{t-1} + i_t * \tilde{C}_t \tag{5}$$

$$O_t = g(W_O \cdot [h_{t-1}, x_t] + b_O) \tag{6}$$

$$h(t) = O_t * tanh(C_t) \tag{7}$$

Three different functions have been used for the activation function g within the LSTM layers using Eq. (8) to (10):

$$relu(R) : R(x) = max(0, x) \tag{8}$$

$$linear(L) : L(x) = mx + c \tag{9}$$

$$tanh(T) : T(x) = (e^x - e^{-x})/(e^x + e^{-x}) \tag{10}$$

LSTM also involves several key parameters such as the number of neurons, the number of iterations in the hidden layer, and the learning rate. These hyper-parameters are typically determined experimentally to optimise the model's fitting ability, training effectiveness, and convergence performance.

C. Performance Evaluation

In this study, the accuracy of the LSTM model's frequency prediction was evaluated by calculating the RMSE between the predicted frequency values and the actual frequency values. The RMSE is a commonly used metric to measure the error between predicted and actual values and it is calculated using Eq. (11), where j is the sample index, N is the total number of samples, $f(x_j)$ is the predicted value of the j^{th} sample and y_j is the actual value of the j^{th} sample:

$$RMSE = \sqrt{\frac{1}{N}\sum_{j=1}^{N}(f(x_j) - y_j)^2} \tag{11}$$

The RMSE provides a quantitative measure of the accuracy of the model's predictions, with a lower RMSE indicating better accuracy. By comparing the RMSE values for different LSTM architectures and parameter settings, the study was able to identify an optimal configuration for frequency prediction.

III. Result Analysis and Discussion

The experimental results were analysed to evaluate the performance of the proposed LSTM frequency prediction model. The analysis involved comparing the predicted frequency values with the actual frequency values obtained from the μPMU data. The RMSE performance metric was applied to quantify the accuracy of the model predictions. The discussion has included an analysis of the impact of the window size, activation function, number of neurons, iterations, and learning rate on the model's accuracy. Overall, the experimental results have provided valuable insights into the effectiveness of the proposed LSTM frequency prediction model.

A. Data Details

For this study, over a 20-day period from March 27 thru April 15, 2023, UK power grid frequency data was obtained from a GDU equipped 8MW solar site in Norfolk, England, that is connected to the UKPN distribution network at 33kV. The GDU's μPMU is providing IEEE C37.118.2-2011 compliant frequency estimations twice per AC cycle (100Hz on a 50Hz electrical system) resulting in a time resolution of 10ms and 6,000 data points per minute.

Over the 20-day period, 65 over or under frequency events were identified that exceeded the operational limits of 49.8Hz - 50.2Hz (also referred to as "pre-fault frequency"). A set of 65 one-minute-long event windows were therefore selected as the LSTM training and testing data for a total of 390,000 data points [4].

B. Comparison and Performance Measures

The dataset was split into three parts for training, validation, and testing, with $2/3$, $1/6$, and $1/6$ of the data applied respectively. Two window sizes (10 and 100 consecutive 10ms data points) were used to train the model and evaluate its performance for two different time horizons (H) of prediction (H10 = 0.1sec and H100 = 1.0sec respectively). The H10 and H100 prediction results for the different activation functions R, L, and T (see Eq. (8), (9), (10) respectively) are shown in Fig. 3. The training RMSE and validation RMSE for H10 are shown in Fig. 3a and 3b, respectively, while Fig. 3c and 3d show the same information for H100. The x-axis represents the number of epochs, and the y-axis represents the RMSE score obtained at the end of each epoch. The results show that for all cases, the tanh (T) activation function performed better than the other two methods, but in the case of H100, the linear (L) function performed comparatively better than T in epoch

10. In both validation phases, the RMSE starts from 0.1 and ends with a value of less than 0.05 for the T function.

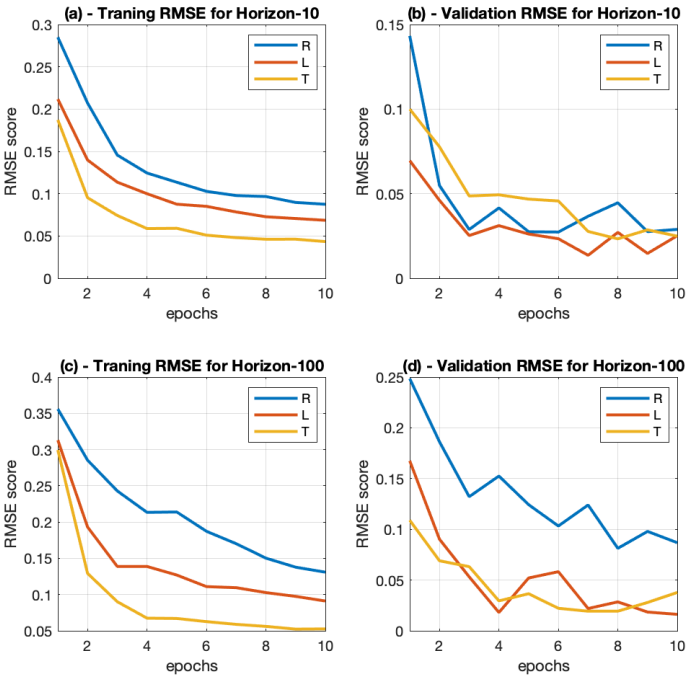

Fig. 3: The RMSE score graph for H10 and H100 for different activation functions.

Table I presents the detailed scores obtained in training and validation for each epoch. It is evident from the table that all the activation functions performed competitively during the validation phase. In the last epoch, L obtained RMSE scores of 0.025 and 0.016 for H10 and H100, respectively, whereas T obtained RMSE scores of 0.025 and 0.038 for H10 and H100, respectively. However, the average validation RMSE scores for R were 0.133 and 0.208, for L, were 0.052 and 0.142, and for T were 0.043 and 0.093 for H10 and H100, respectively. This indicates that the scores for L gradually improved, whereas T remained stable for both training and validation cases. The RMSE scores obtained during testing are listed in Table II. These results are similar to the validation results obtained for the final epochs.

Fig. 4a and 4b chart the actual vs predicted frequency of the test dataset for two different time horizons, demonstrating how the prediction varies with the window size. In the case of R, H10 performs well, whereas for H100 window fails to predict the frequency. Fig. 4c and 4d illustrate that both the H10 and H100 windows are able to predict the frequency, but the shorter time frame ahead H10 is, as expected, more accurate than the H100 for the L method, as the frequency deviates from the actual. On the other hand, the results of T for both the time horizons are quite close to the actual. However, T slightly overestimated the predicted frequency for both time horizons.

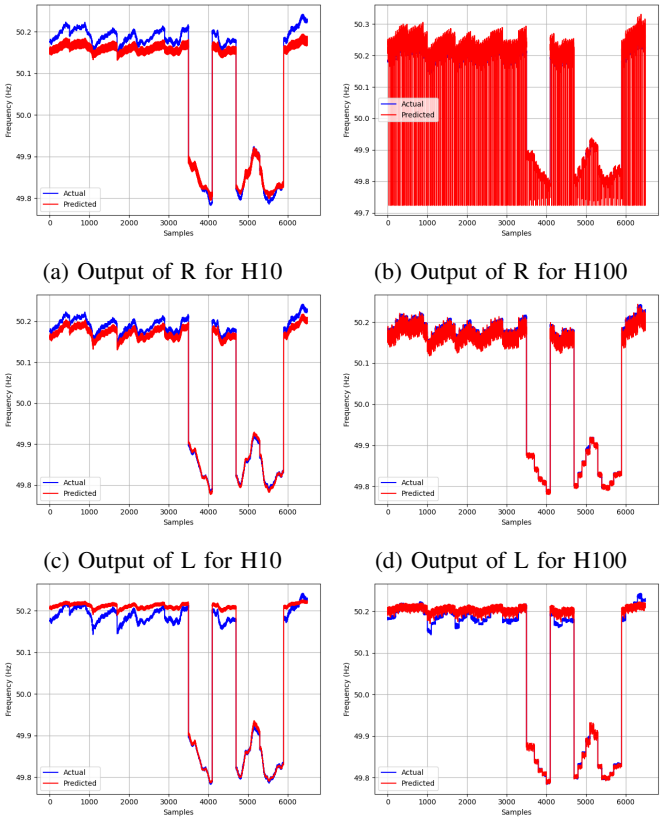

(a) Output of R for H10 (b) Output of R for H100

(c) Output of L for H10 (d) Output of L for H100

(e) Output of T for H10 (f) Output of T for H100

Fig. 4: The output comparison of actual (blue line) vs predicted (red line) frequency over the H10 and H100 horizon between different activation functions.

The proposed model has been trialed against different over-frequency and under-frequency events that exceeded the operational limits (49.8Hz - 50.2Hz) [4]. The model performed well on the 7 non-consecutive days of test data from the same site. The resulting RMSE values between 0.02 - 0.03 indicate the model is able to accurately predict the frequency behaviour of the system 0.1sec and 1.0sec ahead. The results of this analysis demonstrates the significant impact of different activation functions and windowing techniques on the accuracy of the model. This study represents a preliminary investigation into selecting optimal parameters for Neuville's high-resolution (1 data sample per 10 ms) data streams.

The proposed hybrid vector output LSTM model was found to effectively predict the frequency behaviour from the solar site data. Furthermore, this approach can be applied to any power system variables, provided there is sufficient data to train the algorithm.

IV. Conclusion and Future Work

Ensuring grid stability by accurately monitoring and predicting frequency behaviour is crucial to consistent grid operations and avoiding power outages. In this paper, a hybrid vector output LSTM model was used to predict short time ahead

TABLE I: The full training and validation RMSE score for each epoch of different time horizons.

Training Results											
relu (R)				linear (L)				tanh (T)			
Traning RMSE		Validation RMSE		Traning RMSE		Validation RMSE		Traning RMSE		Validation RMSE	
H10	H100	H10	H100	H10	H100	H10	H100	H10	H100	H10	H100
0.285	0.356	0.143	0.248	0.212	0.313	0.070	0.167	0.187	0.299	0.100	0.109
0.207	0.285	0.055	0.186	0.140	0.193	0.046	0.090	0.095	0.129	0.078	0.069
0.146	0.243	0.029	0.132	0.114	0.139	0.025	0.053	0.074	0.090	0.049	0.063
0.124	0.213	0.042	0.152	0.100	0.139	0.031	0.018	0.059	0.067	0.049	0.029
0.114	0.214	0.027	0.124	0.088	0.127	0.026	0.052	0.059	0.067	0.047	0.037
0.103	0.187	0.027	0.103	0.085	0.111	0.023	0.058	0.051	0.063	0.046	0.022
0.098	0.170	0.037	0.124	0.078	0.109	0.014	0.022	0.048	0.059	0.028	0.019
0.097	0.150	0.045	0.081	0.073	0.103	0.027	0.028	0.046	0.056	0.023	0.019
0.090	0.138	0.028	0.098	0.071	0.097	0.015	0.018	0.046	0.052	0.029	0.028
0.087	0.131	0.029	0.087	0.069	0.091	0.025	0.016	0.043	0.053	0.025	0.038

TABLE II: Testing RMSE for horizon-10 and 100 of the three different activation functions.

Testing RMSE		
	H10	H100
relu (R)	0.0284	0.0892
linear (L)	0.0156	0.0184
tanh (T)	0.0207	0.0161

horizons of 0.1sec, and 1.0sec. Further, this model was tested with a longer window of 10.0sec, where the T activation function outperformed among others, achieving RMSE values of (H1000 R) 0.025, (H1000 L) 0.024, and (H1000 T) 0.016 respectively.

The study demonstrates the potential of deep learning models, specifically LSTM-based models, for power grid frequency behaviour prediction, with the importance of selecting appropriate activation functions for optimal results. Further research can explore the model's performance on longer time horizons, different sites, different synchronous grids, and other power system variables by combining multiple input features and modifying the model architecture with more training data for better prediction accuracy and investigating their applicability for power system monitoring and control.

ACKNOWLEDGMENT

This work was jointly funded by London South Bank University and Neuville Grid Data Ltd.

REFERENCES

[1] Gandhi, O., Kumar, D.S., Rodríguez-Gallegos, C.D. and Srinivasan, D., 2020. Review of power system impacts at high PV penetration Part I: Factors limiting PV penetration. Solar Energy, 210, pp.181-201.

[2] Homan, S. and Brown, S., 2020. An analysis of frequency events in Great Britain. Energy Reports, 6, pp.63-69.

[3] Hordeski, M.F., 2020. Emergency and Backup Power Sources:: Preparing for Blackouts and Brownouts. River Publishers.

[4] Mandatory Frequency Response- National Grid ESO, Version 1.1, https://www.nationalgrideso.com/document/92441/download

[5] Boyer, S.A., 1999. SCADA: supervisory control and data acquisition. International Society of Automation (ISA).

[6] A. von Meier, E. Stewart, A. McEachern, M. Andersen and L. Mehrmanesh, "Precision Micro-Synchrophasors for Distribution Systems: A Summary of Applications," in IEEE Transactions on Smart Grid, vol. 8, no. 6, pp. 2926-2936, Nov. 2017.

[7] Dey, M., Rana, S. P., Wylie, J., Simmons, C. V., & Dudley, S. (2022). Detecting power grid frequency events from μPMU voltage phasor data using machine learning.

[8] Sharifzadeh, M., Sikinioti-Lock, A., & Shah, N. (2019). Machine-learning methods for integrated renewable power generation: A comparative study of artificial neural networks, support vector regression, and Gaussian Process Regression. Renewable and Sustainable Energy Reviews, 108, 513-538.

[9] Kruse, J., Schäfer, B., & Witthaut, D. (2020). Predictability of power grid frequency. IEEE access, 8, 149435-149446.

[10] M. B. Djukanovic, D. P. Popovic, D. J. Sobajic et al., "Prediction of power system frequency response after generator outages using neural nets", IEE P-GENER TRANSM D, vol. 140, no. 5, pp. 389-398, 1993.

[11] Zhang, Y., Wang, X., & Ding, L. (2020, August). LSTM-Based Dynamic Frequency Prediction. In 2020 IEEE Power & Energy Society General Meeting (PESGM) (pp. 1-5). IEEE.

[12] Chen, Q., Wang, X., Lin, J., & Chen, L. (2021, April). Convolutional LSTM-based Frequency Nadir Prediction. In 2021 4th International Conference on Energy, Electrical and Power Engineering (CEEPE) (pp. 667-672). IEEE.

[13] Simmons, C.V., Neuville Grid Data Management Ltd, 2021. Methods and apparatus for the sensing, collecting, transmission, storage, and dissemination of high-resolution power grid electrical measurement data. UK patent GB2579156.

[14] Dey, M., Rana, S. P., Simmons, C. V., & Dudley, S. (2021). Solar farm voltage anomaly detection using high-resolution μPMU data-driven unsupervised machine learning. Applied Energy, 303, 117656.

[15] Dey, M., Rana, S. P., Neuville Grid Data Management Ltd, 2022, High-resolution electrical measurement data processing, GB Patent GB2599698B.

[16] Wang, L., Liu, Y., Li, T., Xie, X., & Chang, C. (2020). Short-term PV power prediction based on optimized VMD and LSTM. IEEE Access, 8, 165849-165862.